Mechanics of Contact and Lubrication – ME5656
Department of Mechanical & Industrial Engineering
Northeastern University
Fall 2011

Tribology of Electrical Contacts

Richard Gilley

Northeastern University
360 Huntington Ave.
Boston, MA 02115
gilley.r@husky.neu.edu

ABSTRACT

The electrical contact resistance of a contact pair is a characteristic that strongly influences contact life. Scientists and Engineers have rigorously studied the mechanics behind conductive contacts in order to understand and model their behavior. Of critical importance is accurately modeling electrical contact resistance of rough contact members. An accurate model will lead to robust electrical contact designs and increased life for the given application and scale. Statistical, multi-scale roughness and fractal geometry are a few examples of models that have been created to model electrical contact resistance. These models have been successful in eliminating flaws and building on previous models. As electronic devices become increasingly smaller, there is a need to apply these models to micro and nano-scale contacts. Scientists and engineers will continue to work diligently in modeling electrical contact resistance so that micro and nano-scale devices are as robust as macro scale devices.

1.0 INTRODUCTION

Electronic devices are becoming increasingly important in this technological age. Of particular importance are tribological studies of stationary and sliding electrical contacts. There is an increasing demand for contacts that can withstand higher currents and have a longer service life in the macro and micro scales. As with most electronics, electrical contacts are following the trend of reduced size while requiring equal or better performance. Analyzing electrical contacts on a tribological level has provided insight about the mechanics responsible for friction, wear and lubrication. Tribological characteristics such as these play a role in the electrical contact resistance and contact life. Of equal importance are surface roughness characteristics and how these characteristics contribute to electrical contact resistance. This necessitates the need for accurate models to determine the electrical contact resistance, or ECR, based on a surface profile. Accurate knowledge of ECR can lead to the development of robust designs for the given application and scale. This paper will provide an overview of electrical contacts and review the key contact resistance principles presented by Holm and Greenwood. This will be followed by a review of statistical, multi-scale roughness and fractal geometry models used to predict ECR. This paper will close with a review of open problems in the field and the future state of tribological issues of electrical contacts. It should be noted that this review touches the surface of ECR and is only a brief review of a select group of modeling techniques. There are numerous other modeling techniques to determine ECR and many other factors such as friction, lubrication and wear that contribute to ECR.

2.0 OVERVIEW

Surfaces, when viewed under a microscope, have many defining characteristics that the human eye is unable to see. Surfaces are generally defined by their roughness, which consists of peaks and valleys of varying heights and depths. The peaks and valleys of man-made surfaces are generated by different manufacturing and finishing processes. When two bodies are in contact, the true contact area is significantly less than the nominal contact area [8]. Actual contact takes places at the peaks of the surfaces that are coincident. Two surfaces in intermittent contact that carry electrical current are known as *electrical contacts.* The two electrical conductors are simply know as *contacts;* one being the anode and the other the cathode. Contacts that are electrically connected are referred to as closed contacts. Contacts that are separated so that there is no current flow are referred to as open contacts [5]. The constriction that impedes current flow between electrical contacts is referred to as *contact resistance*. Two basic theories that laid the foundation to contact resistance will be discussed.

2.1 Holm's Theory

Holm's theory laid a foundation from which many other theories have been created. The actual current flow between two contacting surfaces takes places through small circular spots. These surface irregularities that conduct electricity are known as circular a-spots. The current flow lines bend as they pass through a-spots as seen in Figure 1. The restriction of current flow through the small conducting spots leads to constriction resistance which adds to the overall contact resistance [5].

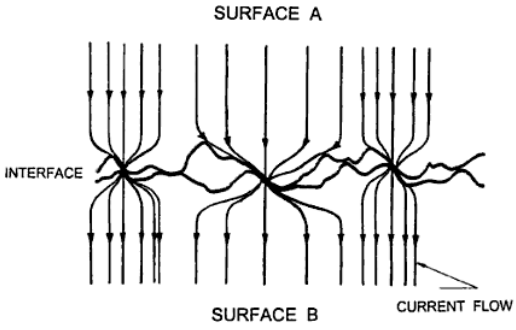

Figure 1 - Current flow through a-spots [8]

Holm used a simple example to describe the basics of his theory. He considers two cylinders, C_1 and C_2 that are in contact with each other. The apparent contact area between the two cylinders is A_a as seen in Figure 2.

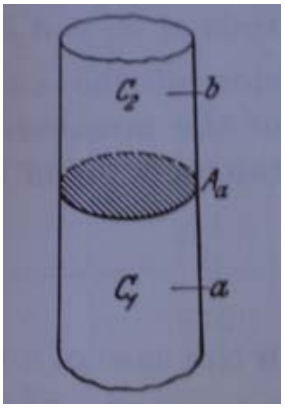

Figure 2 - Holm Contact Resistance Example [8]

In reality the surfaces in contact are rough. The actual contact area, taking into account the roughness of the materials, is defined as A_c. The constriction of current flow through the a-spots leads to the constriction resistance as mentioned earlier. A voltage measurement, U_{ab}, is taken between points *a* and *b* while current is flowing. This allows for calculation of the resistance, R_{ab}, using Ohm's law.

$U_{ab} = IR_{ab}$ [5]

Holm then assumes that the current flows through area A_a. This area is perfectly smooth and does not contain a-spots. A measurement is then taken across points a and b with current flowing to obtain the resistance R^0_{ab}. The constriction resistance, R_c, equals

$R_c = R^0_{ab} - R_{ab}$ [5]

If there is absence of a film resistance on the contact surfaces, then the contact resistance is equal to the constriction resistance. If there are film resistances, then the contact resistance is the sum of the constriction resistance and the film resistance. The contact resistance, R, for contacts of different materials and a film resistance is

$R = R_{c1} + R_{c2} + R_{film}$ [5]

The constriction resistance for one circular a-spot in an electrically conducting pair (Figure 3) of cylinders is

$$R_s = \frac{\rho}{4a} \quad [8]$$

where ρ is the resistivity of the contact material, *a* is the radius of the a-spot and R_s is referred to as the spreading resistance. Therefore, the total constriction resistance, R_c, for two circular a-spots in contact is

$$R_c = \frac{(\rho_1 + \rho_2)}{4a} \quad [8]$$

Formulas also exist for non-circular a-spots. A-spots can also be modeled by using elliptical, rectangular or ring shapes. Holm's theory primarily focuses on contact of single a-spots. In reality, electrical current flows through multiple a-spots. Greenwood expanded on Holm's theory and related constriction resistance to multiple a-spots.

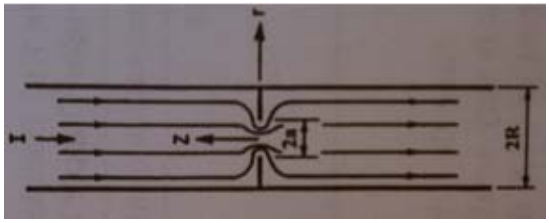

Figure 3 - Current flow through single a-spot [8]

2.2 Greenwood's Theory

Contacting surfaces normally consist of multiple a-spots that act as paths for electric current flow. When two metallic surfaces are coincident, the actual contact takes place at the peaks of the contact asperities. The asperities are most often grouped in clusters or dispersed over the contact surfaces based on the overall surface roughness and waviness profile [8]. The number of a-spots in contact increases as contact force increases. The constriction resistance can be calculated knowing the

size and location of the a-spots. Film resistance can reduce the number of a-spots that actually conduct electricity. This makes is difficult to quantify the number of a-spots in contact. Greenwood's basic equation for contact resistance of a large quantity of a-spots within a single cluster is

$$R = \rho\left(\frac{1}{2na} + \frac{1}{2\alpha}\right) \quad [8]$$

where ρ is the resistivity of the contact material, *n* is the number of circular a-spots, *a* is the mean a-spot radius and α is the radius of the cluster. The cluster radius is also referred to as the Holm radius [8]. The $1/2na$ term is the a-spot resistance and the $1/2\alpha$ term is the cluster resistance.

An array of 76 identical a-spots can be seen in Figure 4. The shaded portion of the figure is a single continuous contact that has an equivalent resistance to the array of 76 a-spots. The outer circle is the Holm Radius, α.

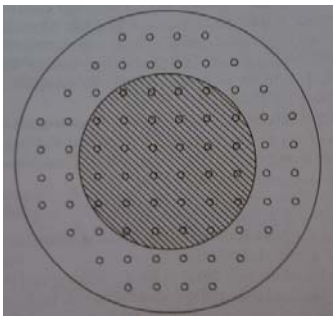

Figure 4 - Array of 76 identical a-spots with Holm Radius (outer circle) and a single continuous contact of same resistance (shaded circle) [8]

Greenwood calculated the effect of the a-spot radius on the a-spot and cluster resistance. The results can be seen in Table 1 along with the Holm radius, α, and the radius of a single spot of comparable resistance. It can be seen that as the a-spot radius increases, the a-spot and cluster resistance decrease. It can also be seen that for an a-spot radius of approximately .05, the cluster resistance is more than the a-spot resistance. The results told Greenwood that the number and distribution of the a-spots does not have a significant effect on the contact resistance [8]. This assumption assumes that the a-spots are evenly distributed and there is no film resistance.

a-Spot Radius	a-Spot Resistance, 1/2na	Holm Radius, α	Cluster Resistance, 1/2α	Radius of Single Spot of Same Resistance
0.02	0.3289	5.34	0.0937	1.18
0.04	0.1645	5.36	0.0932	1.94
0.10	0.0658	5.42	0.0923	3.16
0.20	0.0329	5.50	0.0909	4.04
0.50	0.0132	5.68	0.0880	4.94

Table 1 - Effect of a-Spot radius on resistance [8]

This was confirmed by Nakamura and Minowa who used FEM and Monte Carlo techniques to verify that the distribution does not have a significant effect on contact resistance [8]. Different distributions of a-spots can be seen in Figure 5. The Holm radius is represented by the outer circle and the single equivalent contact is represented by the shaded region.

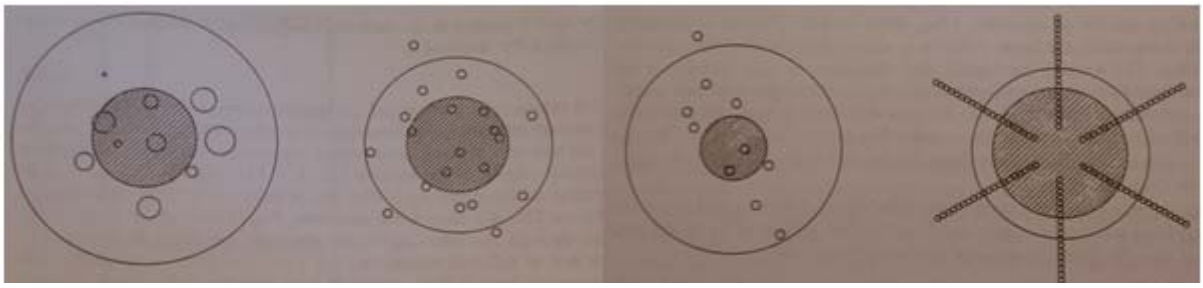

Figure 5- Different a-spot distributions with Holm Radius (outer circle) and single continuous equivalent contact (shaded circle) [8]

3.0 TRIBOLOGY AND ELECTRICAL CONTACT RESISTANCE

Several different models have been devised to describe the characteristics of a rough contact surface and predict ECR. These include multi-scale roughness, fractal and statistical models to name a few. New models are devised to solve a flaw or deficiency seen in a previous model. Advances in measurement tools have displayed fractal and multi-scale surface characteristics that were not seen in the days when statistical modeling techniques were prominent. This has made it difficult to choose a particular model [1]. Models can aid scientists and engineers in designing robust contacts that have increased life and lower ECR. The goal is to devise models that accurately reflect and predict experimental results. The following sections provide a high level review of models used to calculate ECR.

3.1 Multi-scale Roughness Model

The multi-scale roughness model seeks to represent a rough contact surface by using stacked or superimposed sinusoids. Fast Fourier transforms and several other mathematical computations are used to break down each layer of asperities into a representative frequency, which are then stacked upon each other. The multi-scale model is then applied to this data and seeks to find the area and contact resistance of the different frequencies or asperity levels. This is summed over all different levels to find the total contact resistance [9]. A pictorial representation of the stacked sinusoids can be seen in Figure 6.

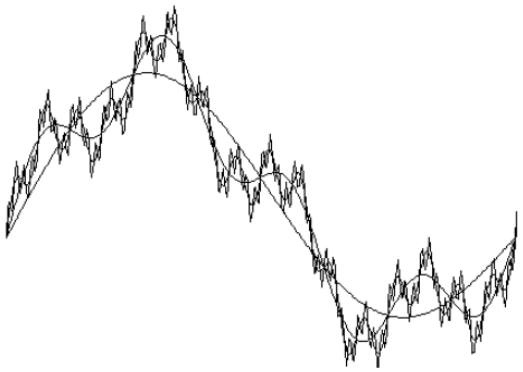

Figure 6 - Surface roughness depicted using superimposed sinusoids [9]

Wilson, Angadi and Jackson's multi-scale model takes into account that elastic-plastic interactions occur between contacting surfaces. Different parameters are used at the point where the loading reaches a critical value and interactions are no longer fully elastic. The multi-scale roughness model predicts the ECR and area for each frequency level *i* [9]. First, the average radius of the contact is calculated for each frequency level.

$$a_i = \sqrt{\frac{A_i}{2*\pi*A_{i-1}*f^2}} \quad [9]$$

A_i is the individual asperity area of contact and *f* is the spatial frequency. The ECR is then calculated using Holm's basic equation for a single asperity along with an alleviation factor, Ψ. Per Holm's theory and the alleviation factor, the electrical contact resistance Er_i, for each asperity level, is

$$Er_i = \frac{\rho_{L1}+\rho_{L2}}{4a_i} * \Psi_i \quad [9]$$

where ρ_L is the resistivity for the contact member materials. For the multi-scale roughness model, the total contact resistance summed over all the frequency levels *i* is

$$Er_{total} = \sum_i^{i_{max}} Er_i * \eta_i * A_i \quad [9]$$

where η is the area density of the asperities.

The researchers of this particular methodology compared the data to statistical methods by using profilometer data of a machined tin surface. The multi-scale roughness model was applied to the surface profile data and plots of the ECR vs. load and real contact area vs. load were obtained.

As seen in the right graph of figure 7, the ECR decreases with increasing contact load. As the load is increased, the individual asperities deform, thus increasing the a-spot radius and real contact area. It can be seen that the elastic-plastic models deviate from the perfectly elastic models. This is due to the increased contact area from plastic deformation. The left graph of figure 7 depicts the ECR vs. non-dimensional load for different surface roughness values. As expected, the rougher the surface the

higher the contact resistance at any given load value. Wilson, Angadi and Jackson have indicated that at very high loads the results of statistical and multi-scale models deviate. Up until that point, the data between the two models is fairly consistent leading them to believe that the multi-scale model is accurate [9]. Work is still needed to identify the root cause of deviations at high loads.

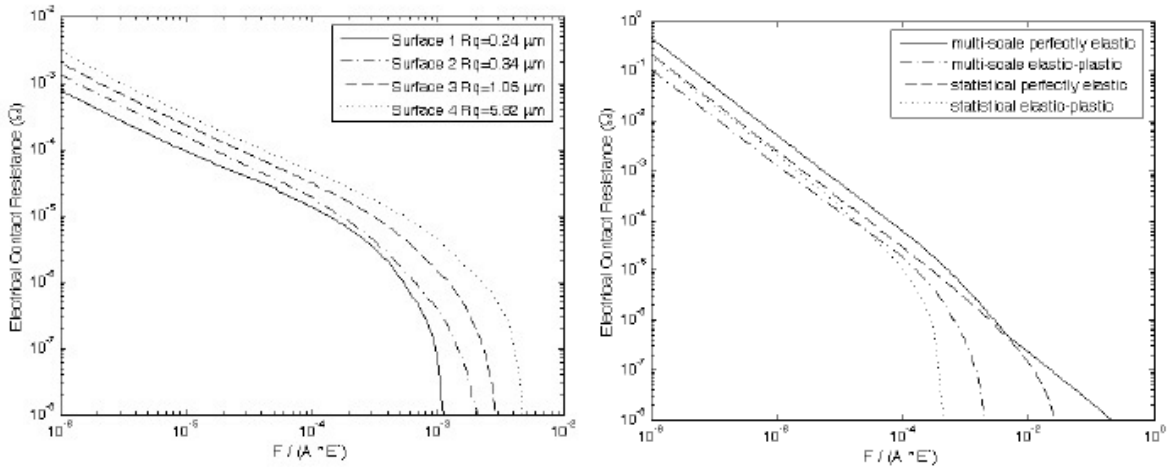

Figure 7 - Electrical contact resistance vs. dimensionless load for a.) different surface roughness values (left) and b.) statistical and multi-scale models (right) [9]

3.2 Statistical Model

Statistical methods have been widely used to represent a rough electrical contact surface. Wilson, Angadi and Jackson compared their multi-scale roughness model to a known statistical model. Background for the statistical model is explained in detail in [4]. For the statistical model, asperity heights are given by a Gaussian distribution Φ, which is equal to

$$\Phi = \frac{(2\pi)^{-1/2}}{\sigma_s} exp\left[-0.5\left(\frac{z}{\sigma_s}\right)^2\right] \quad [9]$$

where σ_s is the standard deviation of the asperity heights. The area and load were then calculated by taking an integral of the above equation. For a perfectly elastic contact situation, the electrical contact resistance Er_e is

$$\frac{1}{Er_e\,(d)} = 2A_n\eta\rho_L^{-1}R^{1/2}\int_d^\infty \omega^{1/2} * \Phi(z) * dz \quad [9]$$

where A_n is the nominal contact area, η is the area density of asperities, ρ is the density of surface material, R is the radius of a hemispherical asperity, E is the elastic modulus, ω is the interference between the hemisphere and the surface and Φ is the distribution function of asperity heights [9].

For an elastic-plastic case that takes into account the deformation of asperities, the electrical contact resistance Er_{ep} is

$$\frac{1}{Er_{ep}(d)} = A_n \eta \int_d^{\infty} \frac{2a_{ep}}{\rho_L} \Phi(z) * dz \quad [9]$$

where a_{ep} is the radius of the area of the elastic-plastic contact. Wilson, Angadi and Jackson use an alleviation factor, bringing the final elastic-plastic ECR to

$$Er = Er_{ep} * \Psi \quad [9]$$

The results of the comparison of the multi-scale roughness model to the pre-existing statistical model can be seen in the right graph of figure 7. The multi-scale and statistical models have comparable data up until high loads are reached as mentioned in the previous section.

3.3 Fractal Geometry Model

A third model presented by Kogut and Komvopoulos uses fractal geometry to characterize a rough surface. Fractal geometry has the advantage of scale invariance. Scale invariance means that the measurements are independent of sample length and instrument resolution. With this model, a 3D surface geometry is created using a modified two-variable Weierstrass-Mandelbrot function [6]. This surface geometry is then used in conjunction with elastic-plastic surface deformation principles and constriction resistance calculations of the micro-contacts. A 3D fractal surface profile can be seen in Figure 8.

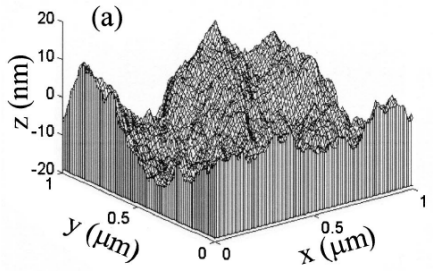

Figure 8 - 3D fractal surface profile [6]

This method seeks to calculate the ECR using the Holm resistance and the Sharvin resistance. The constriction resistance R_c at a particular micro-contact is calculated as

$$R_c = \frac{4(\rho_1+\rho_2)\lambda}{9a} + \frac{\rho_1+\rho_2}{2\pi r}\int_0^{\infty} \exp\left(-\frac{x\lambda}{r}\right)\frac{\sin(\pi x)}{\pi x}dx \quad [6]$$

where ρ is the resistivity of the materials in contact, *a* is the contact area, *r* is the radius of the contact area and λ is the average electron mean free path. For r<λ, this equation reduces to the Sharvin resistance R_S.

$$R_S = \frac{(\rho_1+\rho_2)\lambda}{2a} \quad [6]$$

This is described as ballistic travel of electrons across contact surfaces without scattering. For r> λ, the R_c equation reduces to the Holm resistance R_H

$R_H = \frac{\rho_1+\rho_2}{4r}$ [6]

where scattering is present. The total electrical contact resistance R taking into account all micro-contacts is

$R = \left[\sum_i^{N(a's)} R_{ci}^{-1}\right]^{-1}$ [6]

where R_{ci} is the constriction resistance for the i*th* asperity, and N(a'$_s$) is the number of asperities. R is then converted into a dimensionless value R*.

The results of this study are based on fractal dimension D and fractal roughness G. Fractal roughness G is a height scaling parameter. The surface becomes smoother with a decreasing value of G. The fractal dimension D has to do with high and low frequency components of the Weierstrass-Mandelbrot function. The surface becomes smoother with an increasing value of D [6].

Plots were generated displaying ECR vs. load and contact area for multiple parameters using a fractal surface topography representation generated by this model and elastic-plastic contact mechanics.

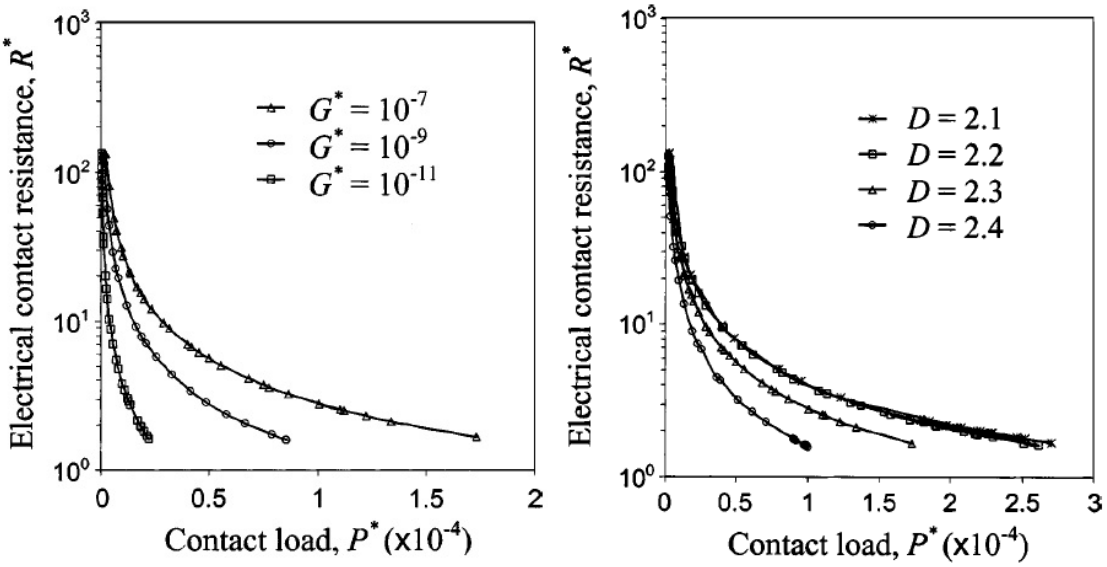

Figure 9 - Electrical contact resistance vs. contact load for a.) different fractal roughness values, G (left) and b.) different fractal dimension values, D (right) [6]

The left graph of figure 9 depicts the ECR vs. the contact load for varying values of the fractal roughness G. As expected the ECR is lower for the surfaces with a lower fractal roughness value. Significantly less contact load is required to achieve an equivalent ECR with a fractal roughness value of $G=10^{-11}$ [6]. This is due to the increased contact area that is associated with a smoother surface.

The right graph in figure 9 depicts ECR vs. the contact load for varying values of the fractal dimension D. The ECR is lower for smaller values of the fractal dimension D. For contact surfaces of

increasing smoothness, the contact area will be greater and the ECR will be lower. The results of this plot are similar to the variation of fractal roughness G [6].

3.5 Open Problems in the Field

A recent model and testing was performed by Read, Land and Slocum to predict the electrical contact resistance in MEMS scale contacts based on the assumption that the current flow lines are restricted more in a thin film contact than a contact on a bulk scale. In particular the spreading resistance is contained in a much smaller area in a thin film contact [7]. A pictorial representation can be seen in figure 10.

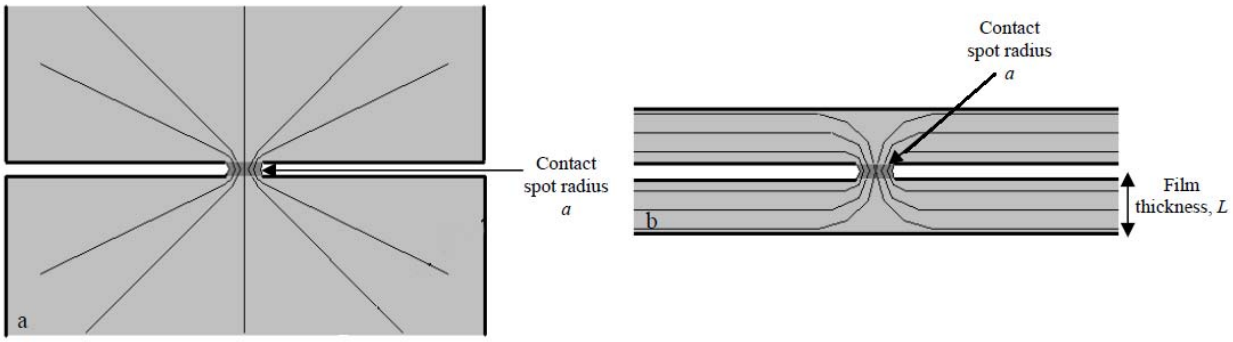

Figure 10 - Current flow lines at a-spot between a.) two macro scale contacts b.) two thin film contacts [7]

Read, Land and Slocum concluded that a reduction in film thickness or an increase in contact spot radius leads to a greater ECR for a/L>1. They also concluded that a reduction in film thickness or an increase in contact spot radius leads to a lower ECR for a/L<1 [7]. They plan to perform more tests to better understand the results and investigate a particular transition area where the contact spot radius exceeds that of the film thickness.

This is one of many examples that portray open work in modeling ECR. It also shows the number of different variables at hand when performing an experiment. Accurately determining the ECR is extremely difficult and involves a significant amount of testing to determine if a model is accurate.

4.0 FUTURE STUDY

Tribology of electrical contacts on the macro-scale has been a focus of scientists and engineers for the past century. When electrical contacts are analyzed on the micro and nano-scale, it becomes increasingly difficult to control friction, wear, lubrication and roughness properties. It is crucial that these properties are controlled in MicroElectroMechanical Systems, or MEMS devices. The methods for

controlling friction, wear and lubrication of macro-scale contacts do not apply to micro-scale contacts [3][7].

In MEMS devices, the dimensions of the contact area are on par with the system dimensions. New tools have been developed in recent decades to cope with the drastic reduction in scale. Atomic force microscopes, 3D contact/non-contact profilometers and optic/untrasonic instruments are now aiding scientists and engineers in analyzing micro and nano-scale surfaces [2]. Advanced computer simulations have also been developed to allow for more comprehensive analyses and visualizations of what is actually going on at this scale. With macro-scale contacts, one can see the system with their eyes or a basic microscope. There is also a significant amount of history that details the study of macro-scale contact design principles and phenomena. Micro and nano-scale contacts are the new frontier of tribology and will be a key player in tribology in the coming decades.

REFERENCES

[1] Barber, J.R. "Surface Roughness and Electrical Contact Resistance." Weblog Entry. iMechanica, web of mechanics and mechanicians. Jan. 10, 2007. Accessed: Nov. 27, 2011. <http://imechanica.org/node/671>

[2] Braunović, Milenko et al. , Electrical Contacts: Fundamentals, Applications and Technology. Boca Raton: CRC Press, Taylor & Francis Group, 2007.

[3] Day, Linda A. "Tribology Frontiers in Electrical Contacts." Tribology & Lubrication Technology. FindArticles.com. 12 Oct, 2011 <http://findarticles.com/p/articles/mi_qa5322/is_200608/ai_n21399326/pg_4/?tag=content;col1>

[4] Greenwood, J.A. and Williamson, J.B.P. "Contact of Nominally Flat Surfaces." Proceedings of the Royal Society of London. Series A, Mathematical & Physical Sciences 295.1442 (1966): 300-319.

[5] Holm, Ragnar. Electrical Contacts - Theory and Application. New York: Springer-Verlag, 1967.

[6] Kogut, L., Komvopoulos, K. "Electrical Contact Resistance Theory for Conductive Rough Surfaces." Journal of Applied Physics 94.5 (2003): 3153-3162.

[7] Read, M.B., Lang, J.H., Slocum, A.H. "Contact Resistance in Flat Thin Films." 2009 Proceedings of the 55th IEEE Holm Conference on Electrical Contacts (2009): 300-306.

[8] Slade, Paul G., Electrical Contacts – Principles and Applications. New York: Marcel Dekker, 1999.

[9] Wilson, Evertt W., Santosh Angadi, and Robert Jackson. "Electrical Contact Resistance Considering Multi-Scale Roughness." 2008 Proceedings of the 54th IEEE Holm Conference on Electrical Contacts (2008): 190-197.